

# Analysis of Rotor-Fuselage Interactions Using Various Rotor Models

David M. O'Brien, Jr.\* and Marilyn J. Smith†  
*Georgia Institute of Technology, Atlanta, GA 30332-0150*

Accurate prediction of the rotor and fuselage interaction is essential for the design and analysis of modern rotorcraft. A variety of Navier-Stokes based methodologies have been employed in the past to simulate these effects. The purpose of this study is to examine the merits of some of the simplified techniques of modeling the rotor and their influence on the physics of the overall rotor/fuselage interaction problem. Specifically, a constant actuator disk, varying actuator disk, and blade element actuator disk are considered. The computational results are compared with wind tunnel data obtained on various rotorcraft models. The constant actuator disk is found to be inadequate for most applications, but can be easily improved upon by allowing for pressure variations about the blade radius and azimuth.

## Nomenclature

$A$	= rotor disk area
$C_T$	= rotor thrust coefficient, $C_T = T / (0.5\rho A\Omega^2 R^2)$
$C_p$	= pressure coefficient, $C_p = p / (0.5\rho V^2)$
$C_L, C_D, C_Y$	= lift, drag, and side force coefficients, respectively, $C_F = F / (0.5\rho V^2 S)$
$C_{MX}, C_{MY}, C_{MZ}$	= roll, pitch, and yaw moment coefficients, respectively, $C_M = M / (0.5\rho V^2 SL)$
$f$	= force
$L$	= reference length
$LHS$	= left hand side matrix from the system of governing equations, $LHS*Q = RHS$
$Q$	= state vector: $Q_{compressible}=(\rho, \rho u, \rho v, \rho w, e)^T$ , $Q_{incompressible}=(p, u, v, w)^T$
$R$	= rotor blade radius
$RHS$	= right hand side vector from the system of governing equations, $LHS*Q = RHS$
$S$	= reference area
$T$	= rotor thrust
$V$	= velocity vector, $(u,v,w)^T$
$x, y, z$	= stream, side, and normal directions, respectively
$\psi$	= blade azimuth angle
$\omega$	= nondimensional vorticity
$\mu$	= advance ratio, $\mu = V / \Omega R$
$\Omega$	= rotor rotational velocity

## I. Introduction

MODERN rotorcraft are subject to some of the most complex flow behaviors encountered by aerospace professionals. The rotation of the rotor blades ensures that a steady state never truly exists. Since the diameter of the rotor can be comparable to the length of the fuselage, typical rotorcraft is subject to unsteady flows over much of the domain of interest. The rotor and fuselage interact in a complex, nonlinear fashion, making it difficult to

---

\* Graduate Research Assistant, School of Aerospace Engineering, M/S 0150, Student Member AIAA.

† Associate Professor, School of Aerospace Engineering, M/S 0150, Associate Fellow AIAA.

Copyright 2005 by David M. O'Brien, Jr. and Marilyn J. Smith. Published by the AIAA with permission.

obtain reliable results from simple, potential flow methods. Much of the aerodynamic research pertaining to helicopters is concerned with the prediction of the main rotor forces and induced velocities. A thorough overview of the research performed prior to 1980 can be found in Johnson<sup>1</sup>. By focusing solely on the main rotor a reasonable estimate of the download forces on the fuselage is obtained, but all of the interactions between the rotor and fuselage are neglected.

One of the first attempts to account for the interaction between the main rotor and fuselage is given in Landgrebe<sup>2</sup>. In this approach a comprehensive rotor code was coupled with a fuselage panel method to study the interaction between the two components. This study showed that fuselage alters the rotor inflow causing an increase in the effective angle of attack of the blades. Many other researchers<sup>3,4,5</sup> have since applied similar singularity methods with varying success to model the main rotor and fuselage interaction. The primary problem with these methods is their inability to model viscous effects and shed vortex structure.

As the availability of computing power increased, attention has shifted to solving the Euler or Reynolds-Averaged Navier-Stokes (RANS) equations for either the main rotor, fuselage, or both components. The use of these equations allows the rotor wake to develop as part of the solution process. However, viscous effects such as drag and flow separation, are not predicted if the Euler equations are utilized. Knowledge of the configuration drag is necessary for making accurate performance calculations, and flow separation is particularly important for predicting the hub – empennage and fuselage – empennage interactions.

In order to predict the complex interactions, a Reynolds Averaged Navier-Stokes (RANS) based method is typically required to resolve these viscous-dominated flows. Two general mesh approaches exist for solving the Euler or RANS equations: structured or unstructured. Most modern codes utilize a structured scheme, since the natural ordering of the nodes reduces the required memory and solution time. However, creating a structured grid can be a time consuming task, taking weeks for very complex configurations. Modern applications of structured meshes for rotorcraft have been successfully applied<sup>6,7</sup> using Chimera and/or overset mesh methodologies. Initial research to apply Cartesian-based structured grid methods is also underway<sup>8</sup>. Recent efforts<sup>9,7</sup> have focused on unstructured techniques, which offer the advantage of reduced grid generation times and are easier to adapt to changing configurations. The main premise behind an unstructured technique is that the additional run time is compensated by the significantly reduced grid generation time.

The most detailed analysis of the rotor-fuselage interaction flow field requires the RANS modeling of the actual unsteady motion of the rotor, as well as a time-accurate analysis of the flow over the fuselage. This approach is capable of capturing the unsteady, three-dimensional behavior of the flow over the blades. However, a rotational and stationary grid must be used, since the rotor is in a dynamic frame and the fuselage is in a static one. One approach is to use overset or chimera grids. This approach was used by Hariharan<sup>10</sup> on a simplified helicopter model and was found to correctly capture the general experimental trends. Another approach is to use a rotating grid block, which shares a sliding boundary with the stationary grid. This approach has previously been used with an unstructured Euler solver by Park and Kwon<sup>9</sup>.

These methods, while the most exact to date, are very CPU and clock time intensive. Many design and analysis needs call for more exact predictions of the fuselage drag, but are content to permit simpler models for the rotor. One of the more applicable approaches is to consider only the time-averaged behavior of the rotor, leading to the concept of an actuator disk. This approach has been used to some success by a number of researchers; two of the more prominent references are Chaffin and Berry<sup>11</sup> and Fejtek and Roberts<sup>12</sup>.

In this study, a steady actuator disk will be utilized in conjunction with a RANS unstructured grid methodology to investigate improved actuator disk models. Since some of these methods have been used by previous researchers, the focus in this work is to analyze the physics of each method, rather than re-validate the methodologies.

## II. Computational Method

### A. Basic Methodology Description

The computational code utilized for this work was FUN3D<sup>13,14</sup> developed at the NASA Langley Research Center. This code solves the RANS equations using unstructured, tetrahedral grids. In order to compute solutions over a broad range of Mach numbers, this code is capable of solving both the compressible and incompressible RANS equations. The incompressible option utilizes the method of artificial compressibility proposed by Chorin<sup>15</sup>. Through the use of artificial compressibility, the incompressible RANS equations are

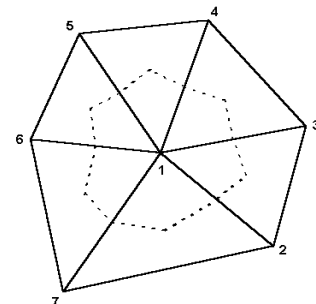


**Figure 1. Control volume for a vertex-based scheme.**

rendered hyperbolic and can be solved in the same manner as their compressible counterparts.

FUN3D uses an implicit, vertex-based finite volume scheme. As shown in Fig. 1, the control volume for this type of scheme has an arbitrary polyhedral shape. Inviscid fluxes are computed at the boundary of each control volume using Roe's flux difference splitting scheme<sup>16</sup>. A second-order accurate, upwind extrapolation is used to determine the values of the flow variables at the boundary. The viscous fluxes are computed in a manner similar to that of a central difference type approximation. Turbulence modeling is achieved by using the Spalart and Allmaras<sup>17</sup> one-equation turbulence model or the two-equation  $k-\omega$  model<sup>18</sup>. The solution is advanced in time using a linearized backward Euler time discretization. The resulting linear system is approximately solved using a point Gauss-Seidel strategy, thereby making use of new information as soon as it becomes available. Through a series of sub-iterations, the approximate solution eventually converges to the exact solution of the exact linear system.

## B. Actuator Disk Fundamentals

In an actuator disk approach, the rotor is represented as an infinitely thin disk capable of sustaining a pressure discontinuity. In reality the actuator disk is a limiting case in which the number of blades goes to infinity. Since a real helicopter only possess a small number of blades, the actuator disk assumption is only useful for obtaining a first estimate of the rotor flow. The most common use of an actuator disk is to simplify the rotor model for analytical (e.g. momentum theory) or simple numerical work (e.g. blade element theory). However, the actuator disk has also been utilized to simplify rotor modeling for different aerodynamic fidelity simulations<sup>11,12</sup>, including more recent Euler- and RANS-based numerical methods<sup>19,20</sup>.

In the literature, actuator disk implementations fall into two general categories: a boundary condition approach and a source term approach. A good survey of these two approaches is presented by Le Chuiton<sup>21</sup>. The primary difference between the two approaches is how the rotor is treated in the fluid control volume. In the boundary condition approach, the control volume is wrapped around the actuator disk in such a way that the actuator disk lies outside of the control volume. Conversely, in the source approach the actuator disk is contained inside the control volume. These differences are illustrated in Fig. 2 using a one-dimensional duct example. A typical internal cell without an actuator disk at face 23 will have the same flux on the left and right sides of the face. For the boundary condition method and source method an actuator disk will be present between cells 2 and 3. The boundary condition method will update the flow variables in the same fashion as the typical internal cell. However, the flux at the actuator disk face will no longer be the same on the left and right sides of the face. Instead, the fluxes are related by some proportionality condition, which in this case is the imposed actuator disk boundary condition. In the source term approach the fluxes are computed just as they were for a typical internal cell, but the update of the flow variables is different. To make the presence of the actuator disk known to the flow solver, an extra source term is added to the equation.

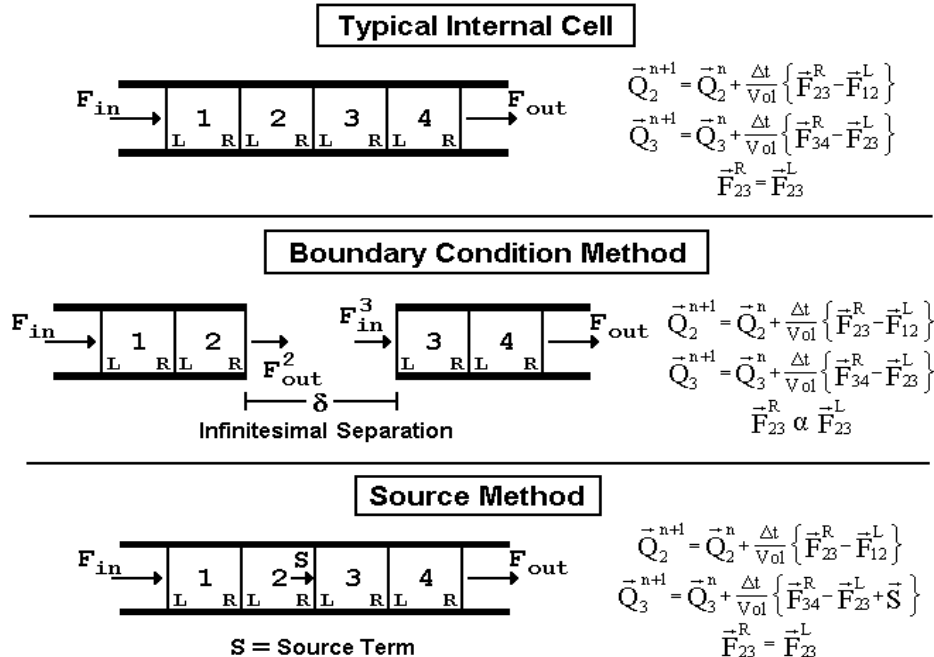


Figure 2. Comparison of the boundary condition and source based actuator disk methods.

Clearly, the boundary condition approach and the source term approach are very similar. In fact, if the proportionality statement is modified to include the source term then the two methods become identical. However, the computational implementation of each of these approaches differs significantly. This difference is particularly noticeable when both methods are implicit (i.e. the flux values are computed at timestep  $n+1$ ). For implicit methods the source method requires significantly less computational effort.

Both methods were tested in the unstructured FUN3D methodology, and the source implementation was found to be more robust when solving the incompressible equations. In addition, the source implementation permits a grid independent rotor definition, that is, rotors do not need to be built into the grid, so that different configurations or rotor motion is simpler.

Two methods can be utilized to introduce the actuator disk sources into the computational domain. In one method the actuator disk surface is defined in the computational grid as the boundary between two sets of cells, allowing both the source method and the boundary condition method to be applied to the same grid. This is the approach that is depicted in Fig. 2. A more generalized approach is to allow the actuator disk to arbitrarily intersect the computational grid. Use of this approach simplifies grid generation, since the disk surface does not need to be incorporated into the grid. Since the main feature of an unstructured approach is to reduce the grid generation time, the generalized method is more appropriate for unstructured methodologies and has been used in this research.

Ideally, the control volumes should feel a force proportional to the area of the actuator disk that intersects the cell. However, FUN3D's use of the dual mesh approach, in which each cell has an arbitrary polyhedral shape, makes the determination of the precise area of intersection a non-trivial task. An alternative approach is to use a discrete approximation as depicted in Fig. 3. The advantage of using a discrete approximation is that the source areas can be rapidly determined, however, it also requires an increased number of sources to obtain the same accuracy. Since the actuator disk is only an approximation of the true rotor behavior, the discrete approximation is utilized for its simplicity.

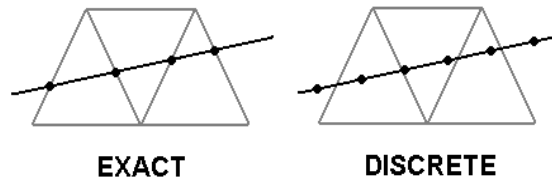


Figure 3. Exact versus discrete source distribution.

The source term is obtained once the force acting on the source elemental area is known. The force is obtained in one of two ways: either a pre-specified distribution (e.g. uniform actuator disk, comprehensive rotor code) or a blade element method, which computes the forces based on the local flow condition. The sources are then added to the LHS and RHS of the governing equations as shown below:

$$\text{LHS} = \text{LHS} + \begin{bmatrix} 0 & 0 & 0 & 0 & 0 \\ 0 & 0 & 0 & 0 & 0 \\ 0 & 0 & 0 & 0 & 0 \\ 0 & 0 & 0 & 0 & 0 \\ 0 & f_x & f_y & f_z & 0 \end{bmatrix} \quad \text{RHS} = \text{RHS} + \begin{bmatrix} 0 \\ f_x \\ f_y \\ f_z \\ \vec{f} \cdot \vec{V} \end{bmatrix}$$

Only the energy equation requires terms on the LHS of the equations. Therefore an implicit incompressible formulation does not require any extra terms to be added to the LHS. Unlike the boundary condition approach, the LHS terms for the source implementation are dominated by zeros, simplifying the computational effort.

The disadvantage of the source approach is that it is a discrete approximation. If the source distribution is too coarse the flow acceleration due to the actuator disk becomes unbalanced, introducing excess vorticity into the flow as shown in Fig. 4.

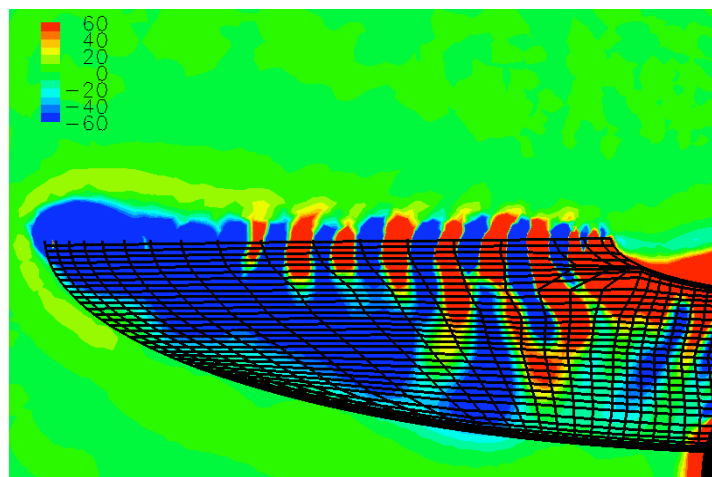
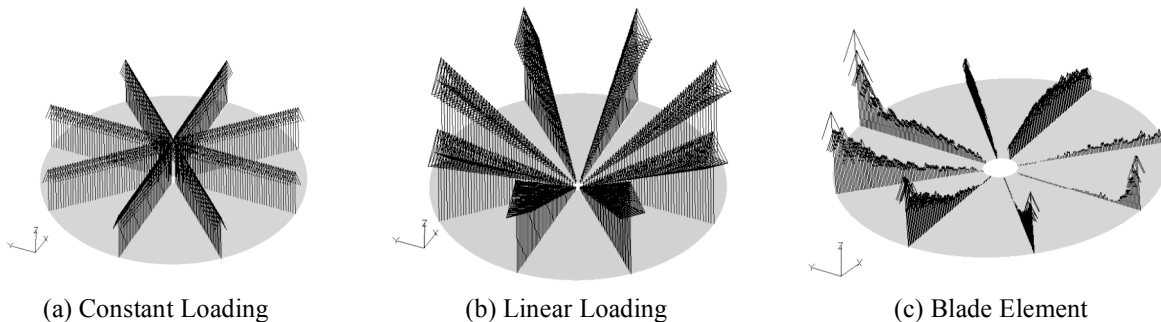


Figure 4. Vorticity generated by a coarse source distribution.

### C. Actuator Disk Loading Models

Four different loading models have been implemented into FUN3D: constant, linear, blade element method, and user specified. The constant and linear distributions are determined using the rotor thrust coefficient. The constant model assumes that the thrust is uniform over the entire disk. The linear model assumes that the thrust varies linear from zero at the hub to a maximum value at the tip. The user specified method allows for the use of rotor loadings from other codes such as a comprehensive rotor code. This method was presented for FUN3D in Renaud<sup>7</sup> and will not be reported in the present work. The blade element method follows the approach used by Chaffin and Berry<sup>11</sup> in which local flow conditions and airfoil lookup tables are used to determine the blade loads. However, in a source model the lift and drag forces are not converted to a pressure. The blade element model is implemented in a loosely coupled fashion in which the blade loads are recalculated at a user specified number of iterations. A visualization of the different blade loading on the actuator disk is show in Fig. 5.



**Figure 5. Comparison of the different loading models, as visualized over the actuator disk.**

### III. Experimental Configurations

Two different experimental configurations are considered in this work. The simplest model (Fig. 6) uses a two-bladed teetering rotor mounted on a cylinder with a semi-spherical cap, which was tested at the Georgia Institute of Technology J.J. Harper Wind Tunnel<sup>22</sup>. The second is the ROBIN<sup>23,24</sup> configuration tested at NASA Langley. This configuration consists of a simple, yet realistic fuselage with a 4-bladed, fully-articulated rotor (Fig. 7). A large body of experimental data is available for this configuration, making it ideal for this study. A third configuration has also been evaluated using a constant actuator disk and a varying pressure based actuator disk found via a comprehensive model for the Eurocopter Dauphin 365N helicopter. The Dauphin results have been previously published<sup>7</sup> and are thus not shown here.

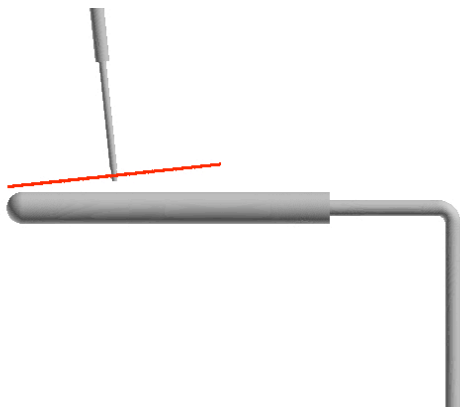


**Figure 6. GT Configuration with actuator disk.**

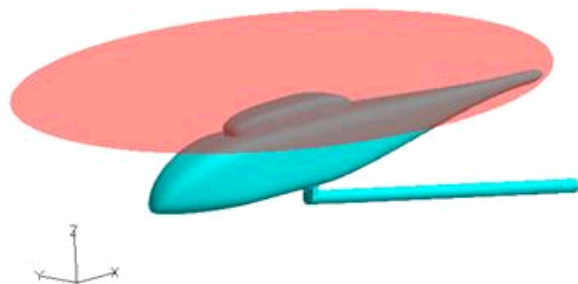


**Figure 7. Robin configuration with actuator disk.**

## IV. Computational Grids

One grid is utilized for each configuration. No attempt was made to find the optimum grid for each configuration, since this was done previously<sup>8</sup>. However, a few grids were generated for each configuration to find a good grid point distribution. The GIT grid consisted of 1.85 million nodes with 59,683 boundary faces on the fuselage surface. The Robin grid consisted of 1.83 million nodes with 107,839 boundary faces on the fuselage surface.

## V. Results

### A. GIT Isolated Fuselage

The Georgia Tech configuration (Fig. 6) is a nominal simple model, but the isolated fuselage pressure coefficient distribution has never been captured by a computational technique. Prior to studying the effects of a rotor on the configuration, an effort to remedy the discrepancy in pressure coefficient was undertaken. The primary reason for the discrepancy is that the rotor shaft and hub have not been modeled in previous studies.<sup>8,20,25</sup> These features lie in close proximity to the fuselage, creating a local blockage in the flow. Therefore, these features need to be modeled to lend credibility to any computational result.

The result of the simulations is shown in Fig. 8. Modeling the configuration without the rotor shaft clearly fails to predict the dip in pressure due to the rotor shaft. When a realistic hub geometry is utilized, a significantly better correlation with the data is obtained. With this model the pressure drop aft of the hub is well predicted, but the pressure prior to the hub is over predicted. One possible explanation for the over prediction is that the simulated hub model is rigid, whereas the realistic hub possessed a flap hinge, which would allow it to deflect from its initial position, but was unfortunately not measured.

The actual hub had a rectangular cross-section, which would rotate in a rotor-on simulation. Since the purpose of this study is to avoid the necessity of modeling rotating grids, the hub was approximated using a cylindrical cross-section, which had a diameter equal to the length of the shorter edge of the real hub. The approximate result is in agreement with the experiment prior to  $X/R=1.0$ , but fails to predict the magnitude and extent of the pressure drop. The reason for this discrepancy is that the approximate hub is more aerodynamic than the exact hub used in the experiment. This reduces the blockage in the flow, causing the pressure drop to be smaller in magnitude and not as influential downstream.

Two observations can be drawn from this relatively simple result:

1. Computational models need to match experimental models as closely as possible.
2. Unstructured methods simplify grid generation, allowing additional features to be easily modeled.

The first observation seems obvious, but is not easy to achieve. Typically experimental results will define the fuselage studied, but neglect sizing information for other features such as the wind tunnel mounting strut, rotor hub, etc. This makes it extremely difficult, if not impossible, to model the same configuration that was tested in the wind tunnel. The second observation is based on the fact that it becomes cumbersome to create extra features when using the more traditional structured grid approaches. Grid generation difficulties and lack of an exact definition are the likely reasons why the rotor shaft and hub have been neglected in the past. This result indicates that it is worthwhile to approximate these features even if the exact definition is not available.

### B. GIT Steady-State Actuator Disk ( $\mu=0.10$ )

The GIT configuration<sup>25</sup> was also tested with an actuator disk. (Note: the approximate rotor hub model described in the previous section is utilized for all actuator disk computations.) The crownline pressure coefficient distributions are shown in Fig. 9. The previous boundary-condition based actuator disk results<sup>8</sup> without the rotor

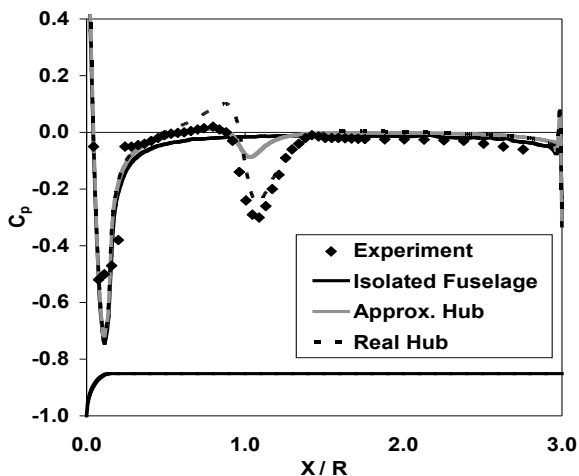


Figure 8. Pressure coefficient distribution along the upper centerline of the GIT configuration.

shaft are shown in Fig. 9a. The new source based actuator disk results are shown in Fig. 9b. The constant model, in both cases, significantly over predicts the pressure in the vicinity of the hub and fails to capture the general trend of the experimental data. This is a direct result of assuming that the loads generated near the hub are the same as the loads generated at the blade tip. The linear variation model assumes a more realistic distribution and thus provides a better correlation with the data. In both cases the linear model predicts a low pressure in the vicinity of the hub and the general trend of the data. By modeling the rotor shaft, the new linear result does a better job predicting the low point under the hub. However, the new model fails to capture the two peak pressures. This is likely a result of the rotor shaft wake interfering with the pressure prediction. Since the discrete source model may be subject to errors due to the source density, a finer source distribution was considered for the linear model. The result was similar to the coarser model except in the nose region. This may be a result of the coarser source distribution smearing out the forward tip vortex. A blade element model was also tested on the finer source grid. The blade element result provides a better correlation with the experimental data than the linear model, since the peak values are better predicted. The poor nose pressure prediction in the blade element model may be due to the fact that the blade flapping was neglected, which would place the forward disk tip in closer proximity to the nose of the fuselage. The new linear and blade element results indicate that the excellent correlation obtained with the previous linear result may have been coincidental.

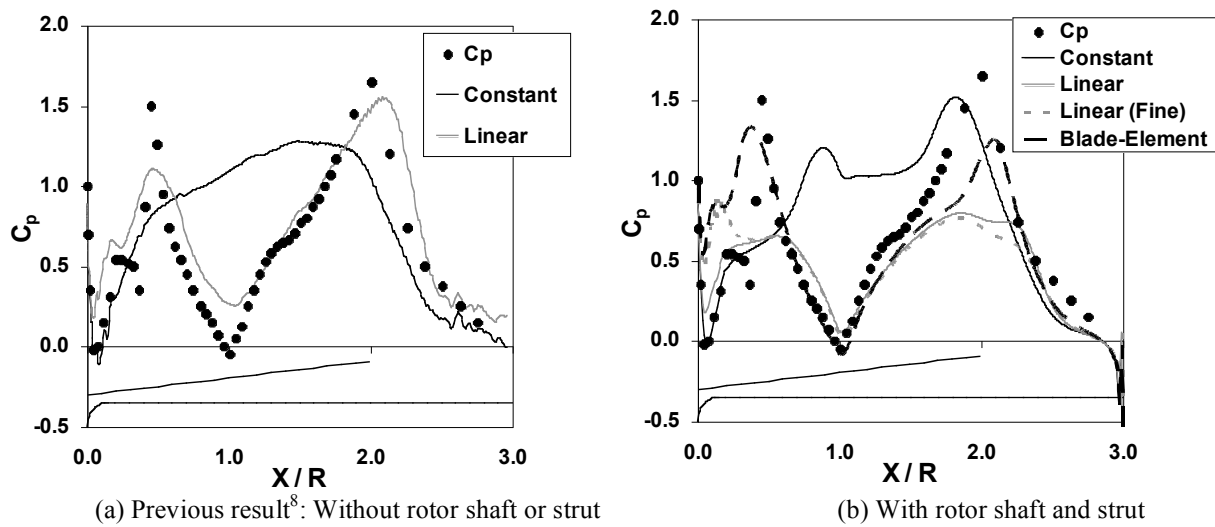


Figure. 9 GIT model with actuator disk.

Symmetry plane pressure coefficient contours are shown in Fig. 10. The region under the hub exhibits a larger pressure for the constant model than the other two. The linear model and blade element model show similar contours. It is interesting to note the location of the rotor wake impingement on the fuselage strut, shown as a high pressure bubble on the upstream side of the strut. The bubble due to the constant model is clearly lower than the other two. This is a result of an increased downwash created by the constant model. The blade element model wake lies in between the constant and linear models. Figure 11 shows the vector plot of velocity. The constant model creates a high pressure region under the entire disk forcing the flow downward. Due to the lower hub pressure the linear model actually exhibits an upwash just aft of the hub. The blade element model shows more of a downwash than the linear model in the aft region of the disk due to a more uniform loading at  $\psi=0$ . This is why the wake impingement on the strut is lower for the blade element model than the linear one. All models exhibit an upwash at the forward disk tip due to the tip vortex convecting downstream.

The behavior of the tip vortex is most clearly seen in Fig. 12 and Fig. 13. Here iso-surfaces of the nondimensional vorticity for  $\omega=10$  (Fig. 12) and  $\omega=5$  (Fig. 13). The strongest vortex due to the rotor is the tip vortex rollup. The constant and linear models look very similar in Fig. 12 except for the hub vortex that appears in the constant model. The hub vortex is a result of the larger hub loadings creating a blade root vortex rollup. Although it is not obvious from Fig. 12c, the blade element model tip vortex is larger on the advancing blade side, due to the larger lift generated by the disk. In Fig. 13 the forward tip vortex is found to travel downstream and hit the fuselage in the vicinity of the forward pressure peak shown in Fig. 10. It can also be seen in Fig. 13a that the vortex is convected downward more rapidly due to the increased downwash of the constant loading.

The resulting fuselage forces are shown in Table 1. The constant model predicts the largest down force and pitching moment on the fuselage than any of the other models. The pitching moment is larger for the constant model as a result of an increased down force over the aft region of the model. Similar trends were also observed in Renaud et al.<sup>7</sup>. This is particularly significant, since a constant model is frequently used as an initial approximation. Using a constant model nearly always over predicts the fuselage downforce in the tail region of a configuration. The downforce due to the linear model is much closer to the blade element model.

These results indicate that the linear model significantly improves the correlation with experiment without increasing the computational complexity, which leads to the conclusion that the linear model should be the first approximation used in Euler or NS based approaches. The constant method is considerably inferior and should only be utilized when comparing with an analytical result using the same assumption. The blade element is naturally appropriate when blade parameters are known, due to its more accurate model of the disk loads.

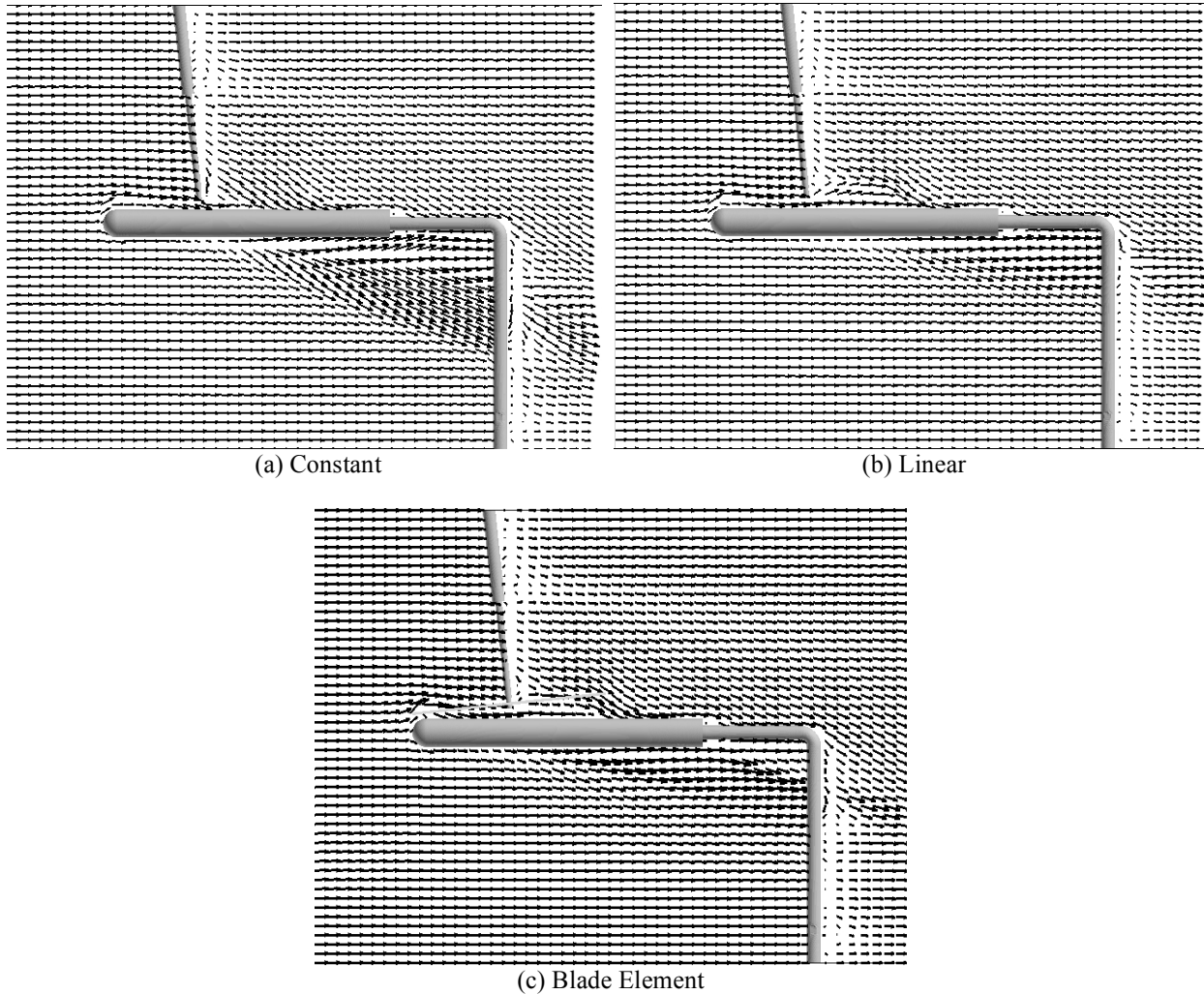


**Figure 11. Symmetry plane velocity vector plots.**

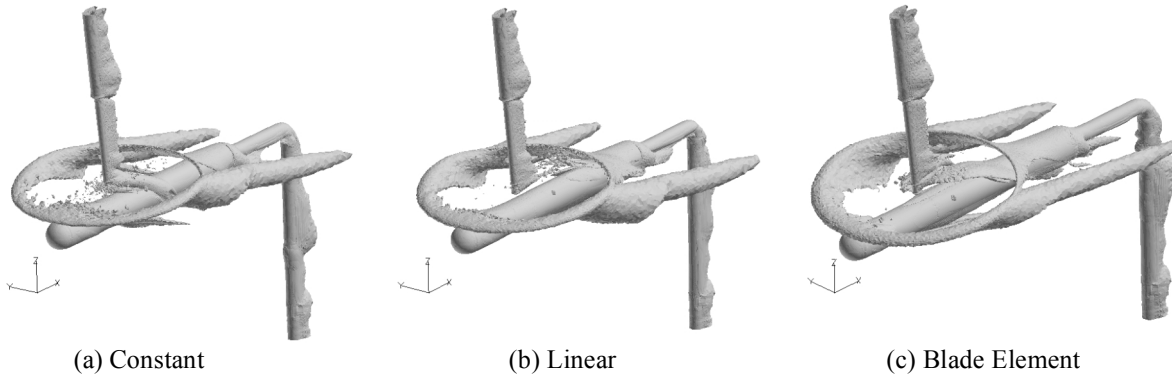


Figure 12. Nondimensional vorticity ( $\omega=10$ ) iso-surfaces.

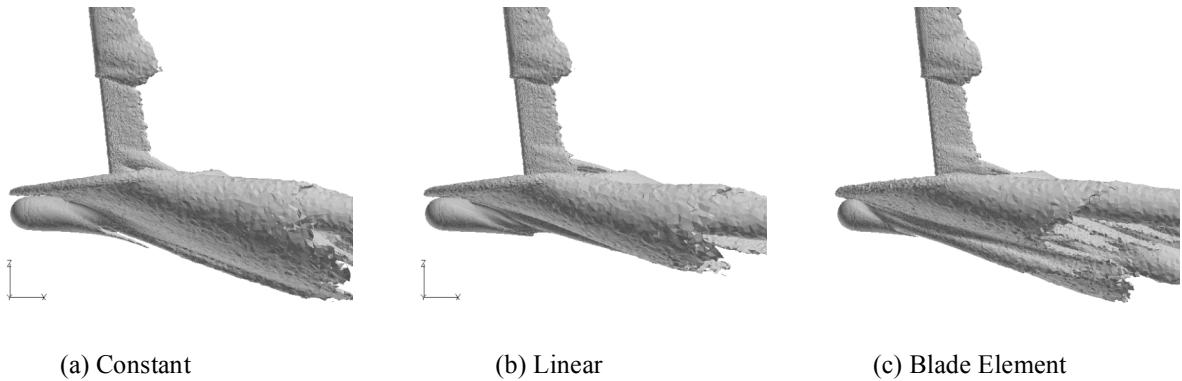


Figure 13. Nondimensional vorticity ( $\omega=5$ ) iso-surfaces.

Table 1. Fuselage forces due to various rotor models.

Load Type	$C_L$	$C_D$	$C_Y$	$C_{MX}$	$C_{MY}$	$C_{MZ}$
Constant	-0.2436	0.0755	0.0075	0.0000	0.0783	0.0128
Linear (Coarse)	-0.1216	0.0703	0.0143	0.0000	0.0211	0.0224
Linear (Fine)	-0.1423	0.0749	0.0000	0.0000	0.0054	0.0070
Blade Element	-0.1669	0.0960	0.1283	-0.0002	0.0376	0.0953

Moment Center = 1,0,0 (Centerline of Fuselage under rotor hub)

### C. Robin Configuration ( $\mu=0.15$ )

Actuator disk data has also been obtained for the Robin configuration using an actuator disk. For this configuration the rotor hub was not modeled and a cutout region was not included in the disk. Select pressure coefficient cross-sections are shown for the constant actuator disk and a linearly varying actuator disk in Fig. 14. The difference between the constant and linear model in Fig. 14a is small in the nose region. Due to the separation distance between the rotor disk and the nose of the fuselage, the freestream flow is the dominant influence over the nose at this advance ratio. In the region of the nacelle the rotor wake influence is significant and the difference between the constant and linear model is clearly illustrated in Fig. 14b and Fig. 14c. The linear model has a much lower pressure in the hub region, giving a better correlation with the experimental data. Over the tail region of the fuselage, the constant model appears to correlate better with the experimental data. Based on the result of the blade element model for the GIT configuration, the zero azimuth tends have a loading closer to that of the constant model. Therefore, it is expected that a blade element model applied to the Robin would exhibit an increased downwash over the tail, which would likely improve the pressure coefficient distribution. Examining the downwash over the disk in Fig. 15 confirms this hypothesis. The experimental result<sup>24</sup> shows a larger downwash region over the aft portion of

the disk, which is closest to that of the constant model. Over the forward portion of the disk the linear model correlates better with the experiment.

Streamlines for the Robin configuration with the constant and linear actuator disk models are shown in Fig. 16. The largest difference between the streamlines is in the region aft of the nacelle. Similar to the result observed for the GIT configuration, the linear loading model exhibits an upwash in the hub region. This indicates a detached flow over the nacelle for the linear model, but the constant loading shows that the streamlines reattach aft of the nacelle.

Iso-surfaces of the non-dimensional vorticity for the Robin are shown in Fig. 17. The linear model is clearly seen to be generating a stronger tip vortex due to the larger tip loads. In Fig. 17b, there is also some vorticity generated in the region of and aft of the hub, although there is no rotor attachment or rotor cutout modeled. The constant rotor creates strong downwash, which when it encounters the narrow portion of the fuselage beneath it, it is merely deflected slightly on its downward path. The linear rotor's downwash is weaker, and when it encounters the fuselage, it interacts with it and creates vertical flow which continues over the rear of the fuselage.

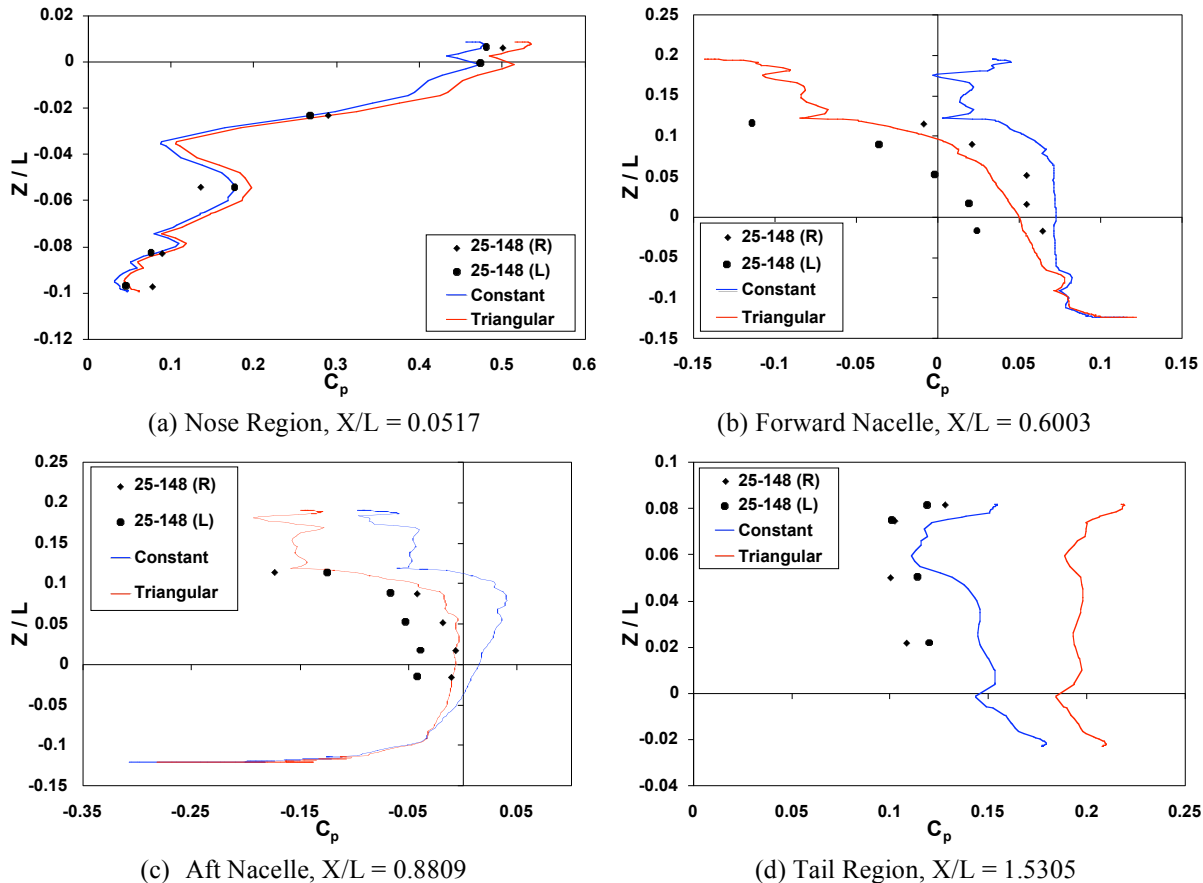


Figure 14. Computed and Experimental Pressure Coefficient on the Robin

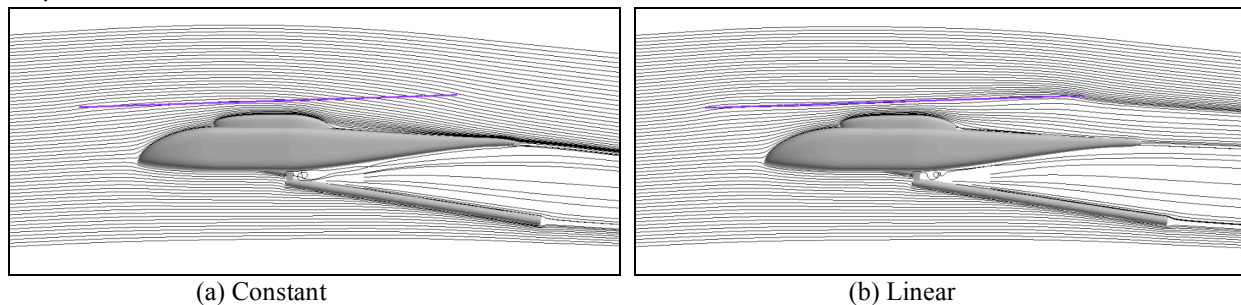
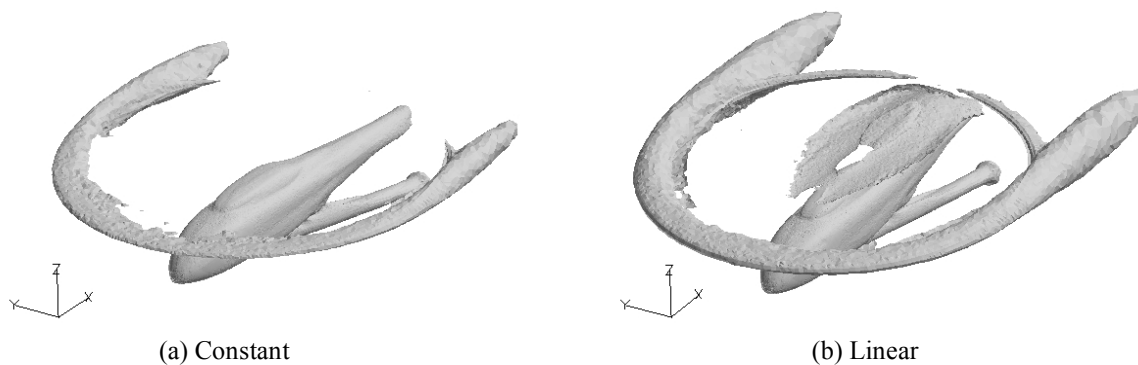


Figure 16. Streamlines for the Robin configuration with actuator disk and strut



**Figure 17. Nondimensional vorticity iso-surfaces ( $\omega=125$ )**

## VI. Conclusion

In this study, an unstructured, tetrahedral solver is utilized to simulate complex rotorcraft flows. Rather than focus on validation of the numerical method used, this paper seeks to enhance the physical understanding of the flows induced by the various actuator disk loading models. It has been found that the simplest approximation that should be considered is a linearly varying (triangular) distribution. The constant approximation possesses a weak physical basis, in that it only considers the total rotor thrust. The linear loading is also based solely on the total thrust but goes one step further by accounting for the variation in local velocity due to the rotation of the blades. The blade element actuator disk is found to be best disk method considered, but requires knowledge of the blade airfoil parameters.

## Acknowledgments

This work is sponsored by the National Rotorcraft Technology Center (NTRC) at the Georgia Institute of Technology. Dr. Yung Yu is the technical monitor of this center. Computational support for the NTRC was provided through the DoD High Performance Computing Centers at ERDC and NAVO through an HPC grant from the US Army, S/AAA Dr. Roger Strawn. The computer resources of the Department of Defense Major Shared Resource Centers (MSRC) are gratefully acknowledged.

## References

- <sup>1</sup> Johnson, W. *Helicopter Theory*, Dover Publications Inc., New York, 1994.
- <sup>2</sup> Landgrebe, A. J., Moffitt, R. C., and Clark, D. R. "Aerodynamic Technology For Advanced Rotorcraft, Parts I and II," *Journal of the American Helicopter Society*, Vol. 22, No. 2-3, 1977.
- <sup>3</sup> Clark, D. R. and Maskew, B. "Study For Prediction Of Rotor/Wake/Fuselage Interference Part I: Technical Report," NASA CR-177340, 1985.
- <sup>4</sup> Mavis, D. N., Komerath, N. K., and McMahon, H. M. "Prediction of Aerodynamic Rotor-Airframe Interaction in Forward Flight," *Journal of the American Helicopter Society*, pp 37-46, October 1989.
- <sup>5</sup> Lorber, P. F. and Egolf, T. A. "An Unsteady Helicopter Rotor-Fuselage Aerodynamic Interaction Analysis," *Journal of the American Helicopter Society*, Vol. 35, No. 3, pp 32-42, 1990.
- <sup>6</sup> Potsdam, M., Yeo, H., and Johnson, W. "Rotor Airloads Prediction Using Loose Aerodynamic/Structural Coupling," *Proceedings of the 60<sup>th</sup> Annual Forum of the American Helicopter Society*, Baltimore, MD, June 2004.
- <sup>7</sup> Renaud, T., Potsdam, M., O'Brien, D. M., and Smith, M. J. "Evaluation of Isolated Fuselage and Rotor-Fuselage Interaction Using CFD," *Proceedings of the 60<sup>th</sup> Annual Forum of the American Helicopter Society*, Baltimore, MD, June 2004.
- <sup>8</sup> Ruffin, S. M., O'Brien, D. O., Smith, M. J., Hariharan, N., Lee, J-D, and Sankar, L., "Comparison of Rotor-Airframe Interaction Utilizing Overset and Unstructured Grid Techniques," AIAA 2004-0046, AIAA 42<sup>nd</sup> Aerospace Sciences Meeting, Reno, NV, Jan. 5-8, 2004.
- <sup>9</sup> Park, Y. M.. and Kwon, O. J., "Simulation of Unsteady Rotor Flow Fields Using Unstructured Sliding Meshes," *American Helicopter Society 58<sup>th</sup> Annual Forum*, Montreal, Canada, June 11-13, 2002.
- <sup>10</sup> Hariharan, N., "High Order Simulation of Unsteady Compressible Flows Over Interacting Bodies with Overset Grids," Ph.D. Thesis, School of Aerospace Engineering, Georgia Institute of Technology, Atlanta, GA, 1995.
- <sup>11</sup> Chaffin, M. S. and Berry, J. D., "Navier-Stokes Simulation of a Rotor Using a Distributed Pressure Disk Method," *American Helicopter Society 51<sup>st</sup> Annual Forum*, Fort Worth, TX, May 9-11, 1995.

- <sup>12</sup> Fejtek, I. and Roberts, L., "Navier-Stokes Computation of Wing/Rotor Interaction for a Tilt Rotor in Hover," *AIAA Journal*, Vol. 30, No. 11, Nov. 1992.
- <sup>13</sup> Anderson, W. K., "Grid Generation and Flow Solution Method for the Euler Equations on Unstructured Grids," NASA TM-4295, 1992.
- <sup>14</sup> Anderson, W. K., Rausch, R. D., and Bonhaus, D. L., "Implicit/Multigrid Algorithms for Incompressible Turbulent Flows on Unstructured Grids," *Journal of Computational Physics*, Vol. 128, No. 2, 1996, pp. 391-408.
- <sup>15</sup> Chorin, A. J., "A Numerical Method for Solving Incompressible Viscous Flow Problems," *Journal of Computational Physics*, Vol. 2, No. 1, 1967, pp. 12-26.
- <sup>16</sup> Roe, P. L., "Approximate Riemann Solvers, Parameter Vectors, and Difference Schemes," *Journal of Computational Physics*, Vol. 43, Oct. 1981, pp. 357-371.
- <sup>17</sup> Spalart, P. R. and Almaras, S. R. "A One-Equation Turbulence Model For Aerodynamic Flows," AIAA Paper 92-0439, 1991.
- <sup>18</sup> Menter, F. R. "Two-Equation Eddy-Viscosity Turbulence Models For Engineering Applications," *AIAA Journal*, Vol. 32, No. 8, pp 1598-1605, 1994.
- <sup>19</sup> Bettschart, N. "Rotor Fuselage Interaction: Euler And Navier-Stokes Computations With An Actuator Disk," Proceedings of the 55<sup>th</sup> Annual Forum of the American Helicopter Society, Montreal, Canada, May 1999, pp 419-438.
- <sup>20</sup> Lee, J. K. and Kwon, O. J. "Predicting Aerodynamic Rotor-Fuselage Interactions By Using Unstructured Meshes," Transactions of the Japan Society for Aeronautical and Space Sciences, Vol. 44, No. 146, pp 208-216, 2002.
- <sup>21</sup> Le Chuiton, F. "Actuator Disc Modelling For Helicopter Rotors," *Aerospace Science and Technology*, Vol. 8, No. 4, pp 285-297, 2004.
- <sup>22</sup> Brand, A. G. *An Experimental Investigation of the Interaction Between A Model Rotor And Airframe In Forward Flight*, Ph.D. Dissertation, Georgia Tech, 1989.
- <sup>23</sup> Freeman, C. E. and Mineck, R. E., "Fuselage Surface Pressure Measurements of a Helicopter Wind-Tunnel Model with a 3.15 Meter Diameter Single Rotor," NASA TM-80051, Mach 1979.
- <sup>24</sup> Elliott, J. W., Althoff, S. L., and Sailey, R. H., "Inflow Measurement Made with a Laser Velocimeter on a Helicopter Model in Forward Flight: Volume I Rectangular Planform Blades at an Advance Ratio of 0.15," NASA TM-100541, April 1988.
- <sup>25</sup> Zori, L. A. J., Mathur, S. R., and Rajagopalan, R. G. "Three-Dimensional Calculations Of Rotor-Airframe Interaction In Forward Flight", Proceedings of the 48<sup>th</sup> Annual Forum of the American Helicopter Society, Washington, DC, June 1992, pp 489-512.

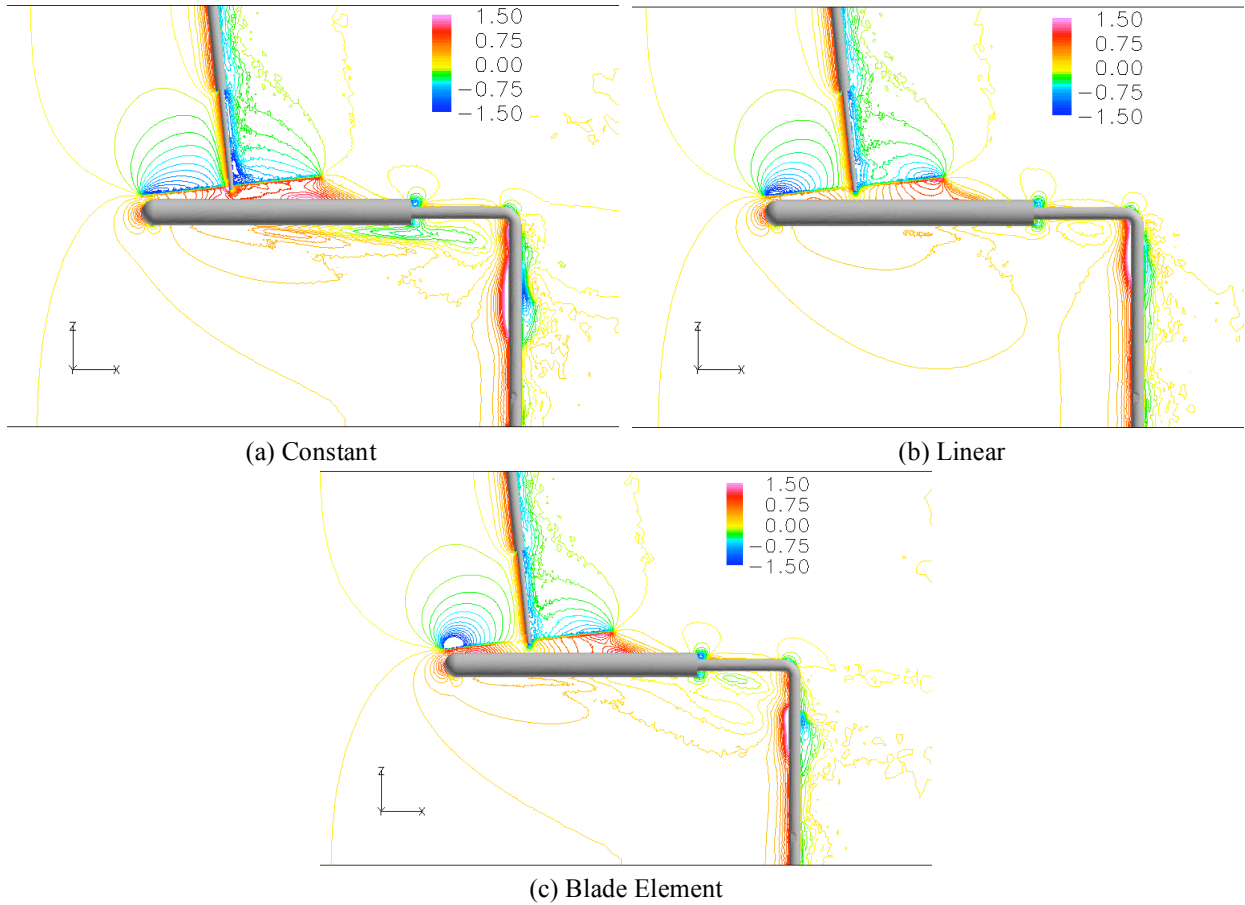


**Figure 10. Symmetry plane pressure coefficient contours**

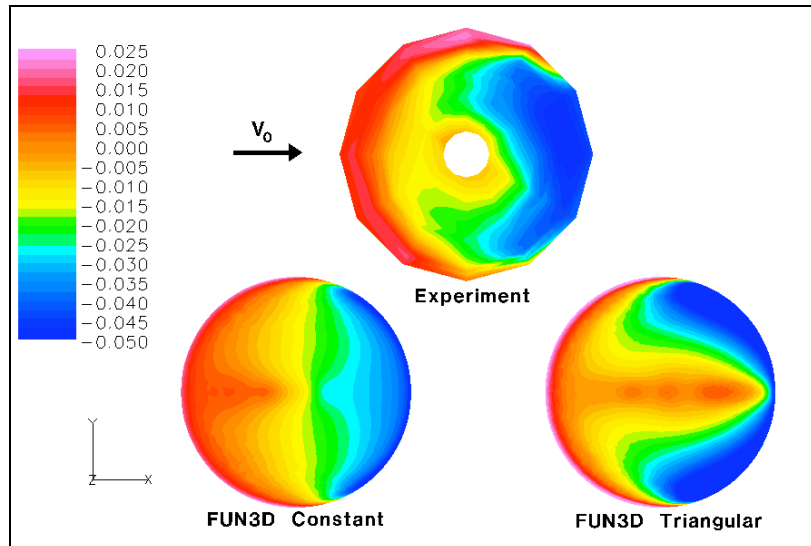


Figure 15. Robin actuator disk inflow compared with experiment